17th World Conference on Earthquake Engineering, 17WCEE
Sendai, Japan - September 13th to 18th 2020

NONLINEAR SEISMIC RESPONSE ANALYSIS OF URBAN UNDERGROUND SUBSTATION

Bo Wen[(1)], Jinxi Yang[(2)], Lu Zhang[(3)], Guanyi Gao[(4)]

[(1)] Professor, Xi'an University of Architecture & Technology, Key Lab of Structural Engineering and Earthquake Resistance, Ministry of Education, State Key Laboratory of Green Building in Western China, wenbo_mail@163.com
[(2)] Post graduate student, Xi'an University of Architecture & Technology, Key Lab of Structural Engineering and Earthquake Resistance, Ministry of Education, 867293813@qq.com
[(3)] Ph.D student, Xi'an University of Architecture & Technology, Key Lab of Structural Engineering and Earthquake Resistance, Ministry of Education, State Key Laboratory of Green Building in Western China, 276537573@qq.com
[(4)] Ph.D student, Xi'an University of Architecture & Technology, Key Lab of Structural Engineering and Earthquake Resistance, Ministry of Education, State Key Laboratory of Green Building in Western China, 269623545@qq.com

Abstract
The seismic fragility performance of underground substation structures with soil-structure-equipment dynamic interaction is investigated using the proposed fragility analysis method for China seismic conditions which is typical of moderate to seismicity regions. Firstly, this study presents the development of a numerical model for using multi-indicators to be used to assess seismic performance of underground substation concrete structures. Then, several groups of ground motion records are selected according to the structural site conditions for incremental dynamic analysis, and the peak ground acceleration is selected as ground motion intensity indicator. In addition, the drift ratio and shear wall plastic drift ratio are taken as structural performance indicators respectively, and the fragility curves of the structure under different indicators are compared. Finally, the seismic fragility of underground substation structure and system are analyzed. The results show that the proposed fragility analysis method can avoid non-conservative estimation that may occur in single-indicator analysis. Thus, the results provided by the proposed method are more conductive to engineering safety.

Keywords: underground substation; electrical equipment; seismic fragility curve; performance indicator; incremental dynamic analysis; correlation coefficient

Introduction

Underground substations are mainly used to supply power to infrastructure and public buildings such as subways, light rails, and large commercial complexes. Ensuring the safety and stability of underground substations under natural disasters such as earthquakes is of great significance for ensuring the normal operation of cities, emergency rescue and reconstruction after disasters. In the past, it was generally believed that underground buildings are more seismic safety due to the restraint of surrounding soil or rocks than the common buildings[1]. However, recent studies of earthquake damage show that underground buildings may suffer severe damage and secondary disasters under the strong earthquakes[2-3]. In view of the low seismic fortification standards and the inadequate seismic design theory of underground bulidings, which resulted in insufficient seismic resistance. In order to reasonably evaluate seismic performance of underground substations, it is necessary to conduct the seismic fragility research on the underground substations.

At present, most researches are focused on the seismic fragility of ground structures[4-6], while few research are focused on that of underground structures. Due to the existence of soil or rocks around the structure, the displacement response of the underground building under the earthquake is generally smaller than that of the ground building, and the dynamic characteristics are also significantly different from those of the ground buildings. Jungwon et al.[7] proposed a fragility analysis method based on quasi-static conditions by comparing the seismic response characteristics of underground box structures under lateral concentrated and distributed loads. Wang Wenhui[8] divided the seismic performance level of underground structure of subways into four levels based on the seismic mechanism of underground structure. Wang Guobo et al.[9] discussed the limit values of the drift ratio of underground structure. Some other scholars[10-11] used vertical bearing members as structural damage indicators and analyzed the seismic fragility of underground frame structures.

Large-scale electrical equipment in underground substation is the weak point suffered earthquakes. In recent real strong earthquakes, the electrical equipment in substations have been damaged severely[12], which has brought great difficulties to the emergency work after the earthquake. However, the current performance-based fragility analysis methods often ignore the damage of equipment inside the structure, and it is difficult to effectively predict the loss of functionality after the disaster. In order to solve these problems, Cimellaro et al.[13] proposed a multi-dimensional fragility analysis method that comprehensively considers structure and equipment damage, and analyzed it in a hospital in California, USA. Liu Xiaoxiao et al.[14] analyzed the impact of the randomness and correlation of multi-dimensional performance indicators on the danger of structural requirements. However, the comprehensive consideration of the seismic requirements of structures and equipment in power systems is still lacking.

Although some achievements have been made on the seismic performance of underground buildings in recent years, there are few studies on the underground substation safety and functionality. Therefore, this paper establishes a finite element calculation model, and the seismic demand model of underground substation is obtained through incremental dynamic analysis[15]. Using the fragility analysis method based on multiple performance indicators, the seismic fragility of underground substation is comprehensively analyzed.

1 Fragility analysis method based on multiple performance indicators

Structural seismic fragility indicates the probability of a structure exceeding or exceeding its performance limit state under earthquakes of different intensities.

$$P_f = P(R \geq r_{\lim} \mid I) \tag{1}$$

Among them, R is the structural response parameter, $r_{\lim}$ is the limit value of the structural limit state, and I is the ground motion intensity.

When considering multiple performance indicators, the fragility is extended from one dimension to multiple dimensions, and its mathematical expression is[16]:

$$P_f = P\left\{ \left(\bigcup_{i=1}^{n} (R_i \geq r_{i,\lim}) \right) \mid I \right\} \tag{2}$$

When considering multiple performance indicators, the structural response R obeys a multivariate log-normal distribution with a probability distribution density of [17]:

$$f(r_1, r_2, \cdots, r_n) = (2\pi)^{-n/2} \, |\boldsymbol{\Sigma}|^{-1/2} \, (r_1 \cdot r_2 \cdot \cdots \cdot r_n)^{-1} \exp[-\tfrac{1}{2}(\ln \boldsymbol{r} - \boldsymbol{\mu})^{\mathrm{T}} \boldsymbol{\Sigma}^{-1} (\ln \boldsymbol{r} - \boldsymbol{\mu})] \tag{3}$$

Where $\ln\boldsymbol{r} = [\ln\boldsymbol{r}_1, \ln\boldsymbol{r}_2, \cdots, \ln\boldsymbol{r}_n]^{\mathrm{T}}$, $\boldsymbol{\mu}$ and $\boldsymbol{\Sigma}$ are the mean vector matrix and covariance matrix of $\ln\boldsymbol{r}$, respectively.When two performance indicators are considered, the above probability distribution density is simplified to a two-parameter case:

$$f(r_1, r_2) = \frac{\exp-(\alpha^2 - 2\rho\alpha\beta + \beta^2)/2(1-\rho^2)}{2\pi r_1 r_2 \sigma_1 \sigma_2 \sqrt{1-\rho^2}} \tag{4}$$

Among them, $\alpha = [\ln(r_1) - \mu_1] / \sigma_1$， $\beta = [\ln(r_2) - \mu_2] / \sigma_2$, and ρ is the correlation coefficient between $\ln(r_1)$ and $\ln(r_2)$.

2 Establishment of finite element analysis model and shake table test verification

2.1 Engineering general situation

The underground substation is a three-layer fully buried frame-shear wall structure. The structural plane size is 50 m × 26.5 m, and the height is 14.7 m. The height of the first underground layer is 5.1 m, the height of the second and third underground layers is 4.8 m, the thickness of the shear wall is 0.8 m, the section size of the frame column is 0.6 m × 0.6 m, the floor thickness is 0.4 m, and the thickness of overlying soil layer is 2 m. Two sets of 110 kV GIS electrical equipment are installed on the second floor of the underground substation structure. Each group includes four cable entry and exit intervals (GIS-1) and one bushing entry and exit intervals (GIS-2). The technical parameters of GIS electrical equipments are shown in Table 1. The layout of the underground substation structure is shown in Figure 1.

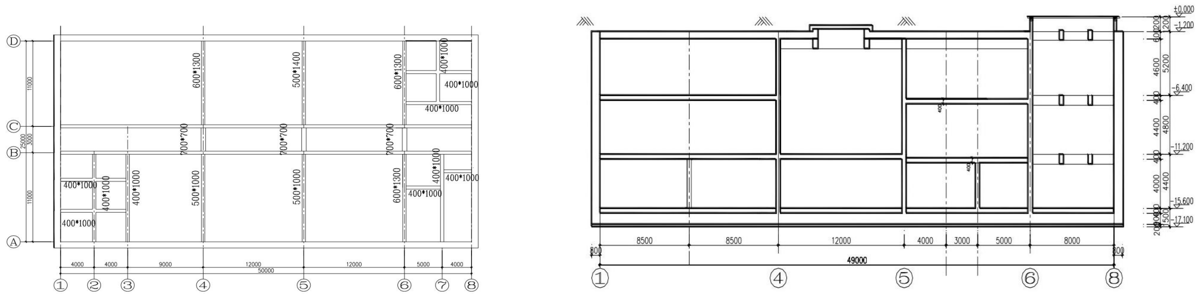

(a) Engineering floor plan(unit: mm) (b) Engineering elevation(Elevation unit: m; measurement unit: mm)

Figure 1 Layout of underground substation structure

Table 1 Technical parameters of GIS

Technical Parameters	GIS-1	GIS-2
structure size/m	7.2×1.5×4.9	15×1.5×5.6
Shell wall thickness/mm	20	20
shell material	aluminum	aluminum
Monomer mass/t	8.6	11
Earthquake resistance/g	0.50	0.50

Table 2 Parameters of soil

Soil	Density /(kg·m^{-3})	Shear wave velocity/(m·s^{-1})	Poisson's ratio	Thickness /m
Plain fill	1720	240.81	0.39	4.30
New loess	1600	317.74	0.30	6.20
Silty clay	1950	321.79	0.30	1.70
Pebble	2250	508.04	0.15	2.10
Silty clay	1950	321.79	0.30	27.0
Coarse sand	1920	504.88	0.26	4.50

2.2 Finite element model

ABAQUS finite element software is used to build a three-dimensional model of the soil-underground substation structure-electric equipment dynamic interaction system, as shown in Figure 2. The size of the foundation soil model is 150 m × 80 m × 45 m. Soil parameters are shown in Table 2. In the seismic dynamic analysis of underground structures, it is inevitable to encounter the problem of how to simulate infinite ground. The currently widely used solution is to intercept a finite range of near-field calculation areas from infinite ground. In the calculation area, numerical methods such as finite element are used to convert the field equations and physical boundary conditions into discrete space-time equations of motion to simulate wave motion. It is transformed into mathematical algebraic operation to realize the numerical simulation of earthquake action[18]. Among the various artificial boundary theories, the viscoelastic artificial boundary[19] is widely used in theoretical research and practical engineering because of its good robustness and relatively simple setting method.

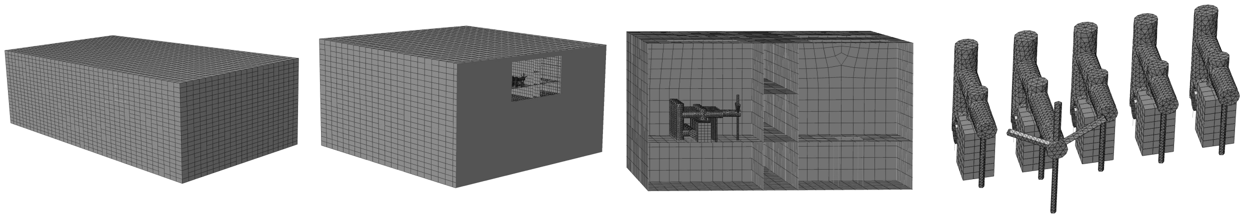

(a) Soil model (b) Soil longitudinal 1/2 section (c) Structure longitudinal 1/2 section (d) GIS Electrical Equipment Group

Figure 2 FEM of soil-structure-equipment interaction system

A three-dimensional viscoelastic artificial boundary is set up around the soil and the bottom surface, and use "hard contact" to simulate the normal action of the structure and the soil contact surface, that is, consider the contact and separation between the ground soil and the underground structure contact surface. Normal pressure can only be transmitted in the contact state. When there is a gap between the contact surfaces, the normal pressure disappears. Friction contact is used to simulate the tangential effect between the contact surfaces, and the friction coefficient is 0.22. In order to improve the calculation efficiency, the floor slab and shear wall of the underground substation structure are simulated by shell elements, the beams and columns are simulated by beam elements; the main body and casing parts of GIS electrical equipment are simulated by shell elements, the bottom brackets are simulated by beam elements, and the switch cabinets are by solid elements simulation.

2.3 Shaking table test of underground substation

The prototype of the shaking table test is a two-story, two-span cast-in-situ reinforced concrete frame-shear wall structure. The plane size of the structure is 20 m × 10 m, the thickness of the overlying soil is 2 m, the height of the first underground layer is 3.75 m, the height of the second underground layer is 6.25 m, and the column spacing is 5 m. The electrical equipment is two sets of 110 kV GIS equipment, which are arranged on the negative second floor of the structure. Particulate concrete is used to simulate the concrete in the original structure, iron wires are used to simulate the steel bars in the original structure, plexiglass is used to simulate the main parts of the electrical equipment such as disconnectors, circuit breakers, AC transformers. PVC is used to simulate the casing parts of the electrical equipment.

Considering the shaking table size of Xi'an University of Architecture and Technology (China), determine the geometric similarity constant of the model S_l = 1/25 and the geometric similarity constant of the device S_l = 1/15. According to the performance parameters of the shaking table, the acceleration similarity coefficient *Sa* of the soil body and the structure is determined to be 1.25, and the acceleration similarity coefficient *Sa* of the equipment is 2.08. The stress similarity constant is determined according to the concrete strength relationship that can be realized in the laboratory, and the stress similarity relationship is adjusted according to the measured values of the strength and elastic modulus of the particulate concrete and galvanized iron wire. Finally, the stress similarity constant of the soil and structure is obtained as $S_\sigma = S_E = 0.075$, the stress similarity constant of the equipment is obtained as $S_\sigma = S_E = 0.045$. According to the dimensional coordination principle, the density similarity constant S_ρ = 1.5 of the soil and structure required for the dynamic test and the density similarity constant S_ρ = 0.324 of the equipment are determined. The produced test model is shown in Figure 3.

(a) Model structure (b) Equipment layout (c) Layered shear box

Figure 3 Testing models

Table 3 Testing cases

structure	PGA/g	Seismic wave input sequence
Prototype structure	0.035→0.07→0.14→0.2→0.4→0.62	El Centro wave→Taft wave→Artificial wave
Model structure	0.04375→0.0875→0.175→0.25→0.5→0.775	El Centro wave→Taft wave→Artificial wave

El Centro wave, Taft wave and an artificial wave were selected as input seismic waves. The test loading conditions are shown in Table 3. Based on the results of the shaking table test and the numerical analysis of the finite element, the rationality of the finite element model is compared and analyzed from the aspects of acceleration response and drift ratio. Due to space limitations, this article only takes the dynamic response of various parts of the structure under the 8 degree rare earthquake as an example. The regulars of other earthquakes are similar. Table 4 and Table 5 show the comparison between the acceleration amplification factors and the drift ratio between the structural layers. It can be seen from the analysis of the data in Table 4 and Table 5 that the results of shaking table tests and numerical analysis have a certain discrete type, and the errors may come from the material constitutive and actual deviations in the finite element model, connection between soil-structure- electrical equipment and construction stages. However, in general, the results of the shaking table test are close to the results of the finite element simulation, which proves the correctness of the finite element model.

Table 4 Comparison of acceleration amplification factor

position	El Centro wave		Taft wave		Artificial wave	
	simulation	test	simulation	test	simulation	test
B1 floor	1.13	1.25	1.10	1.13	1.25	1.11
B2 floor	1.00	1.10	1.06	1.09	1.11	1.11
Electrical Equipment	1.14	1.18	1.21	1.14	1.21	1.45

Table 5 Comparison of drift ratio

position	El Centro wave		Taft wave		Artificial wave	
	simulation	test	simulation	test	simulation	test
B1 floor	1/384	1/323	1/321	1/352	1/402	1/344
B2 floor	1/502	1/447	1/425	1/411	1/514	1/447

2.4 Selection of input seismic wave

In order to consider the uncertainty of ground motion, 15 earthquake records were selected from the strong earthquake database of the US Pacific Earthquake Research Center (PEER). The relevant information of the selected seismic records is shown in Table 6. Amplify each seismic record to generate ground motion records with the peak accelerations of 0.1 g, 0.2 g, 0.4 g, 0.6 g, 0.8 g, 1.0 g, and 1.2 g, respectively. In this way, 105 seismic acceleration records are obtained as input to the vulnerability analysis.

Table 6 List of earthquake records

Number	Earthquake name	Record station	Year	M_w
1	Taft	Taft Lincoln School	1952	7.36
2	Southern Calif	San Luis Obispo	1952	6.0
3	Imperial Valley-05	El Centro Array #9	1955	5.4
4	Northern Calif-04	Ferndale City Hall	1960	5.7
5	San Fernando	Hemet Fire Station	1971	6.61
6	El Centro	El Centro Array #1	1979	6.53
7	Nahanni	Site 3	1985	6.76
8	Loma Prieta	Dublin-Fire Station	1989	6.93
9	Cape Mendocino	Eureka-Myrtle&West	1992	7.01
10	Landers	Boron Fire Station	1992	7.28
11	Northridge	Elizabeth Lake	1994	6.69
12	Kobe	FUK	1995	6.9
13	Duzce	Galata Kop.	1999	7.14
14	Kocaeli	Afyon Bay	1999	7.51
15	Chi-Chi	CHY016	1999	6.2

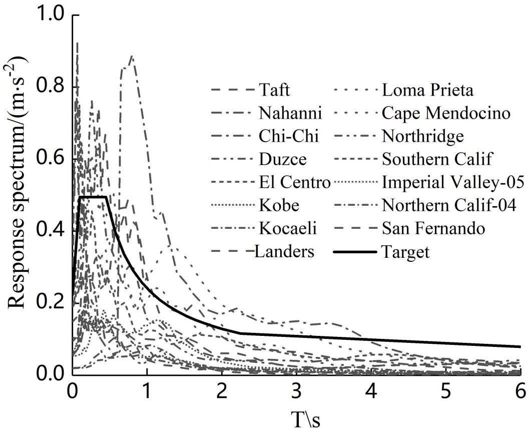

Figure 4 Response spectrum of selected seismic waves

3 Probabilistic seismic capability analysis

3.1 Determination of performance indicators

Performance-based seismic analysis methods require structures with different failure states under different performance goals. Therefore, reasonable selection of ground motion intensity index and damage index is the basis of fragility analysis [20]. When selecting the damage index, comprehensive consideration should be given to the deformation performance of the structure and components to obtain a more accurate analysis result. The drift ratio as a performance index can better reflect the main damage reason and performance level of the structure under the action of earthquakes and has been widely used in scientific research and engineering practice. Shear wall is the main lateral resistance and vertical load-bearing member of underground substation structure, and its deformation capacity can be measured by the plastic drift ratio. Therefore, this paper uses the drift ratio (θ) and the shear wall plastic drift ratio ($\theta_{shear\ wall}$, θ_{sw}) as the structural performance indicators.

Whether an underground substation can operate normally is not only related to the safety level of the structure, but also depends on the working status of the electrical equipment. Because the equipment is more sensitive to acceleration, the peak acceleration of electrical equipment is selected as the equipment performance index, and the limit is set to 0.5 g according to the technical parameters of Table 1.

In the seismic analysis of structures, the peak ground acceleration (PGA) is generally used as the index of ground motion intensity. However, recent studies have shown that the seismic damage of underground structures has a strong correlation with the peak ground velocity (PGV) [21]. Because there is no consensus on the selection of ground motion intensity indicators, this article uses PGA and PGV as ground motion intensity indicators, respectively, and obtains the IDA curves of the structure and equipment response under each index through finite element calculations, as shown in Figures 5 and 6.

It can be seen from Fig. 5 and Fig. 6 that during the whole seismic response process, the degree of dispersion of the IDA curve obtained by using PGA as the ground motion intensity index is lower than the degree of dispersion when using PGV. In order to quantify the degree of discreteness of the structural response data, it is assumed that the ground motion intensity and structural response obey the log-normal distribution[22], and calculate the average logarithmic standard deviation of the structural response corresponding to each index. It can be seen from Table 7 that the average logarithmic standard deviation value corresponding to PGA is small, and the degree of data dispersion is low. Therefore, in this paper, PGA is selected as the index of ground motion intensity in subsequent fragility analysis.

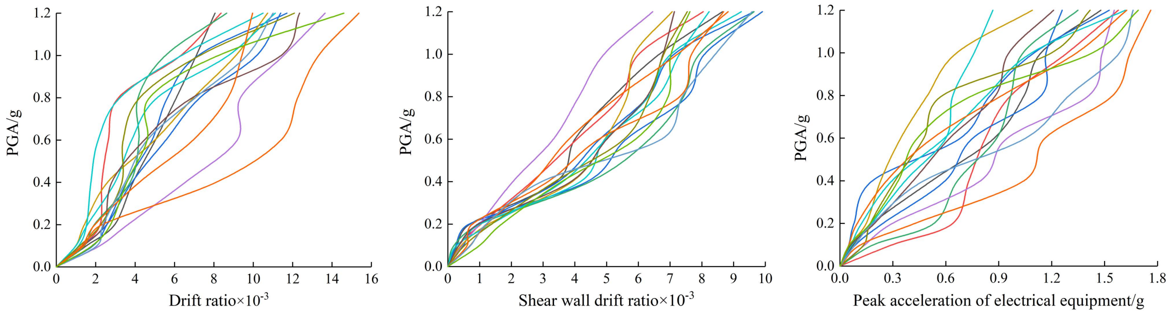

(a) PGA-θ (b) PGA-θ_{sw} (c) PGA-a

Figure 5 IDA curves with PGA as IM

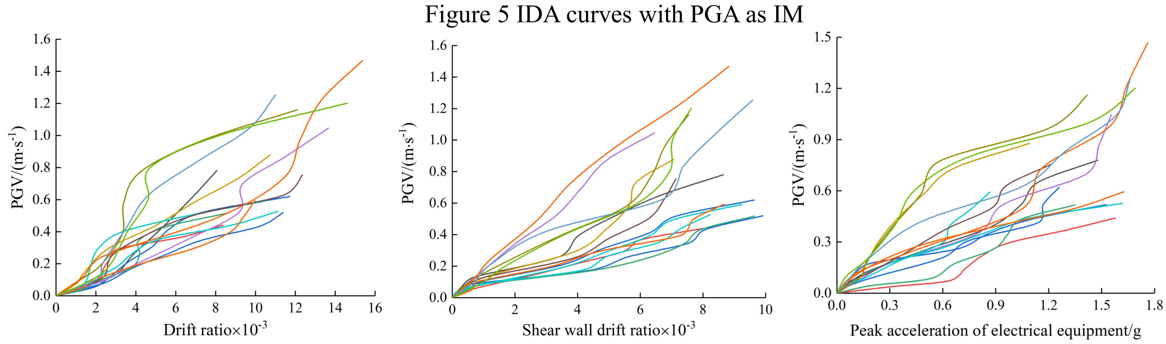

(a) PGV-θ (b) PGV-θ_{sw} (c) PGV-a

Figure 6 IDA curves with PGV as IM

Table 7 Average of logarithmic standard deviation

IM	drift ratio	shear wall plastic drift ratio	Peak acceleration of electrical equipment
PGA	0.304	0.221	0.389
PGV	0.323	0.254	0.401

3.2 Division of performance limit states

This paper refers to China 's seismic design code for buildings[23] and FEMA 445[24]. The seismic performance level of underground substation structures are divided in five levels: basic intact, minor damage, moderate damage, severe damage and collapse, whose performance limit states are corresponded to operational (OP), immediate occupancy (IO), life safety (LF) and collapse prevention (CP).

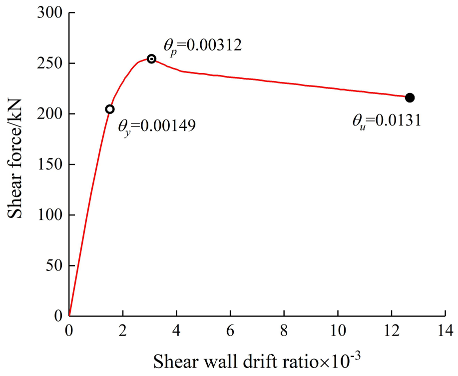

Figure 7 Deformation capacity curve of shear wall

The capacity curve of shear wall is shown in Figure 9, in which θ_y represents the proportional limit, θ_p represents the yield limit, and θ_u represents the deformation limit. The limit plastic drift ratio of shear wall and thedrift ratio of structure are shown in Table 8 and Table 9 [25-28].

Table 8 Thresholds of shear wall drift ratio

Performance level	OP	IO	LF	CP
θ_{sw}	0.001	0.003	0.006	0.009

Table 9 Thresholds of drift ratio

Performance level	OP	IO	LF	CP
θ	1/600	1/300	1/150	1/60

4 Seismic fragility analysis

4.1 Fragility analysis based on single parameter

The fragility curves of underground substation are shown in Figure 8. As PGA increases, the exceeding probabilities corresponding to four limit states gradually increase as well. When PGA is between 0.1g and 0.2g, the exceeding probability curve corresponding to operational (OP) limit state is more obvious, and the structure is slightly damaged. When the PGA is in the range of 0.2g to 0.6g, the increase trend of exceeding probability curve is more obvious and the structure damage changes from slight to moderate. However, when PGA exceeds 0.9g, the exceeding probability corresponding to the limit state for collapse prevention (CP) is still less than 0.1, which means the seismic performance of underground substations are overestimated obviously.

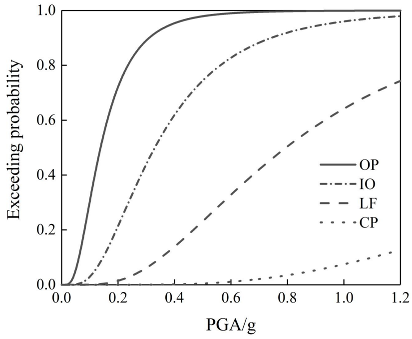

Figure 8 Fragility curves based on drift ratio

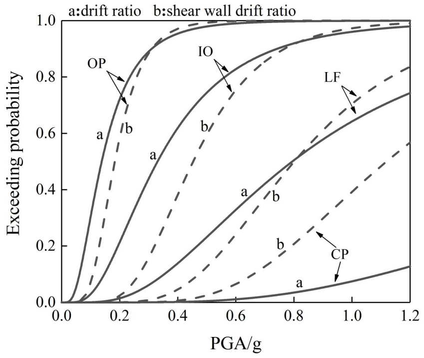

Figure 9 Comparison of seismic fragility curves

Figure 9 shows a comparison chart of seismic fragility curves obtained by taking the drift ratio and the shear wall plastic drift ratio as performance indicators, respectively. Under OP and IO limit states, the exceeding probabilities obtained by drift ratio as the performance index is greater than those obtained by shear wall plastic drift ratio, and the values of the two curves are relatively close to each other. Under the limit of LF, the exceeding probabilities of drift ratio as the performance index is greater than those of shear wall plastic drift ratio when PGA is less than 0.8g. The deformation of the shear wall is the main cause of the underground substation during severe damage and collapse. Therefore, the damage of shear wall should be paid more attention.

4.2 Fragility analysis based on two parameters

Considering drift ratio θ of the structure and plastic drift ratio θ_{sw} of the shear wall as independently. Combining Tables 8 and Table 9 to get the two-parameter vulnerability curve of the underground substation, as shown in Figure 10. Table 10 shows the exceeding probabilities calculated based on different performance indicators under the limit of LF.

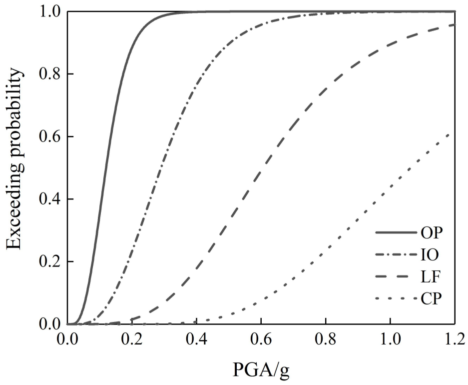

Figure 10 Fragility curves based on two parameters

Table 10 Exceeding probability for different indicators

PGA/g	0.2	0.4	0.6	0.8	1.0
θ	0.015	0.139	0.328	0.504	0.642
θ_{sw}	0.001	0.045	0.241	0.498	0.704
Two parameter	0.016	0.178	0.490	0.751	0.894

When PGA is less than 0.1g, the minor damage probabilities of underground substation is less than 0.4, and the probabilities of other damage levels tends to zero, which is basically in a safe state. When PGA is greater than 0.7g, the structure is severely damaged. The probability exceeds 0.65 and there is a risk of collapse. It can be seen from Table 10 that exceeding probability calculated based on the two-parameter calculation is greater than those of single-parameter method, which indicats that the fragility analysis method based on multiple performance indicators is more conducive to project safety.

© The 17th World Conference on Earthquake Engineering

5 Conclusions

In order to analyze the seismic fragility of urban underground substations, a three-dimensional finite element model considering soil-structure-equipment dynamic interaction was established. Firstly, based on the incremental dynamic analysis method, the seismic response data of multiple groups of underground substation structures and electrical equipment are obtained. Then the drift ratio, the shear wall plastic drift ratio and the peak acceleration of electrical equipment are used as performance indicators to analyze the seismic fragility of underground substation structures and systems. The main conclusions of the study are as follows:

(1) The principles of ground motion intensity and performance indicators applicable to underground substations are proposed.

(2) The drift ratio and shear wall plastic drift ratio are selected as performance indicators and the seismic fragility curves of underground substation is obtained. When the earthquake intensity is small, the safety of underground substation is mainly affected by the structure deformation. With the severe of structural damage, the deformation of shear wall has gradually become the main factor affecting the safety of underground substations.

(3) The seismic fragility analysis method of underground substations based on multiple performance indicators is more conducive to engineering safety than that of single indicator.

Acknowledgements

The authors wish to acknowledge their gratitude towards the National Natural Science Foundation Project (No.51578450) (in China), International cooperation projects of Shaanxi Province (No. 2019KW-047) (in China) and Shaanxi Province Housing and Urban Construction Technology Research and Development Project of China (No.2015-K145).

References

[1] Du Xiuli, Kang Kaili, Xu Zigang, et al. Main characteristics and rules of seismic response for underground structures. *China Civil Engineering Journal*, 2018, 51(7): 11-21. (in Chinese)

[2] Yoo D G, Jung D, Kang D, et al. Seismic Hazard Assessment model for urban water supply networks. *Journal of Water Resources Planning and Management*, 2016, 142(2): 04015055.

[3] Chen Guoxing, Chen Su, Du Xiuli, et al. Review of seismic damage, model test, available design and analysis methods of urban underground structures: retrospect and prospect. *Journal of Disaster Prevention and Mitigation Engineering*, 2016, 36(1): 1-23. (in Chinese)

[4] M. Bhandari, S. D. Bharti, M. K. Shrimali, et al. Seismic fragility analysis of base-isolated building frames excited by near- and far-field earthquakes. *Journal of Performance of Constructed Facilities*, 2019, 33(3): 04019029.

[5] Su Ningfen, Xin Zhuo, Bai Guoliang, et al. Incremental dynamic analysis of high-rise shear wall structure based on shaking table test. *Journal of Building Structures*, 2018, 39(07): 76-83. (in Chinese)

[6] Liu Yang, Li Hongnan, Li Chao, et al. The study on the vulnerability of the concrete stilled steel tubular frame with buckling-restrained braces structure under the coupling of wind and earthquake. *China Civil Engineering Journal*, 2019, 52(02): 56-65. (in Chinese)

[7] Jungwon Huh, Quang Huy Tran, Achintya Haldar, et al. Seismic Vulnerability Assessment of a Shallow Two-Story Underground RC Box Structure. *Applied Science*, 2017, 7(7): 735.

[8] Wang Wenhui. Research on practical seismic analysis methods and performance index of underground structures. Beijing: Tsinghua University, 2013. (in Chinese)

[9] Wang Guobo, Xie Weiping, Sun Ming, et al. Evaluation method for seismic behaviors of underground frame structures. *Chinese Journal of Geotechnical Engineering*, 2011, 33(4): 593-598. (in Chinese)

[10] He Zhiming, Chen Qingjun. Vertical seismic effect on the seismic fragility of large-space underground structures. *Advances in Civil Engineering*, 2019, 9650294: 1-17.

[11] Zhang Wenyang, Abdoul R Ghotbi, Elnaz E. Seylabi, et al. Fragility based seismic performance assessment of buried structures, 5 th *Geotechnical earthquake engineering and soil dynamics conference*, Austin, 2018: 184-192.

[12] Xie Qiang, Ma Guoliang, Zhu Ruiyuan, et al. Shaking Table Test Research on Earthquake Response Mechanism of a Transformer-bushing System. *Proceedings of the CSEE*, 2015, 35(21): 5500-5510. (in Chinese)

[13] Cimellaro G P, Reinhorn A M. Multidimensional performance limit state for hazard fragility functions. *Journal of Engineering Mechanism*, 2011, 137(1): 47-60.

[14] Liu Xiaoxiao, Wu Ziyan, Wang Qiang. Probabilistic seismic demand analysis based on multi-dimensional performance limit states. *Journal of Vibration and Shock*, 2017, 36(01): 181-187. (in Chinese)

[15] Alireza Mohammadi, Atorod Azizinamini, Lawrence Griffis, et al. Performance assessment of an existing 47-story high-rise building under extreme wind loads. *Journal of Structural Engineering*, 2019, 145(01): 04018232.

[16] Casciati F, Cimellaro G, Domaneschi M. Seismic reliability of a cable-stayed bridge retrofitted with hysteretic devices. *Computers & Structures*, 2008, 86(17-18): 1769-1781.

[17] Wang Qiang, Wu Ziyan, Jia Zhaoping. Multi-dimensional fragility analysis of bridge system under earthquake. *Engineering Mechanics*, 2013, 30(10): 192-198. (in Chinese)

[18] Bipin K Gupta, Dipanjan Basu. Timoshenko beam theory-based dynamic analysis of laterally loaded piles in multilayered viscoelastic soil. *Journal of Engineering Mechanics*, 2018, 144(09): 04018091.

[19] Kakar R, Kakar S. Love wave in a voigt-type viscoelastic heterogeneous layer overlying heterogeneous viscoelastic half-space. *International Journal of Geomechanics*, 2017, 17(01): 06016009.

[20] Zhou Changdong, Wang Guopeng, Tian Miaowang, et al. Partitioned seismic vulnerability assessment of hyperbolic cooling tower under multi-dimensional earthquakes. *Journal of Harbin Institute of Technology*, 2017, 49(06): 156-163. (in Chinese)

[21] Chen Zhiyi, Wei Jianshu. Correlation between ground motion parameters and lining damage indices for mountain tunnels. *Natural Hazards*, 2013, 65(3): 1683–1702.

[22] Liu Tong, Chen Zhiyi, Yuan Yong, et al. Fragility analysis of a subway station structure by incremental dynamic analysis. *Advances in Structural Engineering*, 2017, 20(7): 1111-1124.

[23] GB 50011-2010. Code for seismic design of buildings. Beijing: China Architecture & Building Press, 2010. (in Chinese)

[24] FEMA 445. Next-generation performance-based seismic design guidelines. Washington DC: FEMA, 2006.

[25] FEMA 356. Pre-standard and commentary for the seismic rehabilitation of buildings. Washington: Federal Emergency Management Agency, 2000.

[26] Ji Jing, Xiao Xinyu, Cui Jidong, et al. Seismic safety assessment of frame-shear wall structures based on deformation. *Journal of Building Structures*, 2015, 36(S2): 62-69. (in Chinese)

[27] Wen Bo, Niu Ditao. Seismic vulnerability analysis for the main building of the large substation. *China Civil Engineering Journal*, 46(02): 19-23. (in Chinese)

[28] Wen Bo, Zhang Lu, Niu Ditao, et al. Soil-Structure-Equipment interaction and influence factors in an underground electrical substation under seismic loads. *Applied Science*, 2017,7(10):123-145.